Investigation of liquid film behavior at the onset of flooding during adiabatic counter-current air–water two-phase flow in an inclined pipe

Deendarlianto [a], Akiharu Ousaka [b,*], Akira Kariyasaki [c], Tohru Fukano [d]

[a] *Graduate School of Engineering, The University of Tokushima, 2-1 Minami Josanjima, Tokushima 770-8506, Japan*
[b] *Department of Mechanical Engineering, The University of Tokushima, 2-1 Minami Josanjima, Tokushima 770-8506, Japan*
[c] *Department of Chemical Engineering, Fukuoka University, 8-19-1 Jyonan-ku, Fukuoka 814-0180, Japan*
[d] *Department of Mechanical Engineering, Kurume Institute of Technology, 2228-66 Kamizu, Kurume, Fukuoka 830-0052, Japan*

Abstract

The liquid film characteristics at the onset of flooding in an inclined pipe (16 mm i.d. and 2.2 m in length) have been investigated experimentally. A constant electric current method and visual observation were utilized to elucidate the flow mechanisms at the onset of flooding. Two mechanisms are clarified to control the flooding in lower flooding and upper flooding, respectively. The lower flooding occurred at lower liquid flow rate and high pipe inclination angle. In this mechanism, the liquid film does not block the pipe cross-section. On the other hand, the upper flooding occurred at higher liquid flow rate and low pipe inclination angle. In this case, blocking of the pipe cross-section by large wave and entrainment plays an important role. The experimental data indicated that there was no reversal motion of liquid film at the onset of flooding during the operation of both lower flooding and upper flooding. The effects of pipe inclination angle on the onset of flooding are also discussed.
© 2005 Elsevier B.V. All rights reserved.

Keyword: Rhodococcus equi

1. Introduction

Flooding phenomena have been studied in order to develop analytical models to predict the onset of flooding velocity. As a result, a large number of correlations have been proposed in the literature to predict it for a given set of conditions. In spite of the large number of reported results, there is still considerable uncertainty concerning the phenomena at the onset of flooding.

Imura et al. (1977) suggested that the initiation of flooding is due to the instability in the flow that causes a wave to grow rapidly until it bridges the tube cross-section. On the other hand, Karimi and Kawaji (2000) reported that at the onset of flooding, the interfacial

* Corresponding author. Tel.: +81 88 656 7375;
fax: +81 88 656 9082.

E-mail address: ousaka@me.tokushima-u.ac.jp (A. Ousaka).

Nomenclature

C	constant in Eq. (2)
C_W	wave velocity (m/s)
D	inner diameter (m)
f_W	wave frequency (Hz)
g	gravitational acceleration (m/s^2)
J_G	superficial air velocity (m/s)
J_L	superficial liquid velocity (m/s)
J_K^*	Wallis dimensionless number of superficial velocity
L	pipe length (m)
m	constant in Eq. (2)
P_G	air inlet pressure (kPa)
t	time (s)
x	distance from the liquid outlet (m)

Greek letters

η	liquid hold-up
θ	inclination angle from horizontal (°)
ρ_k	liquid and gas density (kg/m^3)

waves do not block the tube and do propagate downward with a considerable velocity. This conclusion is in agreement with the result obtained by Zabaras and Dukler (1988) whose investigation did not reveal the presence of upward moving waves at the onset of flooding. While, Suzuki and Ueda (1977) and McQuilland and Whalley (1985) reported that flooding occurred when large waves, formed near the liquid outlet, are swept upwards by the gas phase.

It is noticed that almost all the studies were performed in vertical pipes and a little work has been reported on the interfacial behavior at the onset of flooding in counter-current two-phase flow in an inclined pipe. Barnea et al. (1986) conducted experiments in the cases of various inclined pipes in which liquid injection was at the mid section. Flooding was detected visually and defined as that the liquid was carried upward to the liquid inlet. They reported that at moderate and high liquid flow rates, flooding occurred as a result of turbulence at the water inlet when porous injection was used. Meanwhile, at low liquid flow rates, the occurrence of flooding was considered as the result from interfacial instability along the pipe. Furthermore, they noticed that the inclination angle of the pipe had dis-

tinct effect. At a given liquid velocity, gas velocity at the onset of flooding increased and then decreased as the inclination was changed from vertical to horizontal. More recently, Mouza et al. (2003) investigated the effects of tube diameter and liquid properties on the onset of flooding in inclined small diameter tubes with inclination angles ranging from 30° to 60°. They reported that the gas velocities at the onset of flooding by Barnea et al. tend to be significantly higher. It is noticed that, in these researches the behavior of liquid film at the onset of flooding in inclined pipes has received little attention. Probably, this is because of difficulties in taking experimental measurements due to the extreme small film thickness and random formation of the interfacial waves in the counter-current flow.

One of the shortcomings of proposed flooding mechanisms is the fact that the onset of flooding is determined subjectively. That is, identification of onset of flooding was often made, for example, by using visual observation or recorded video images, and this may account for large discrepancies among reported flooding data.

The purpose of the present experiment was to use the instantaneous liquid hold-up data, which were measured at seven axially different locations, each 215 mm apart along an inclined pipe, in order to investigate the mechanisms of the onset of flooding. In this experiment, a constant electric current method (CECM) was applied to detect the instantaneous liquid hold-up in adiabatic counter-current two-phase flow. This method is capable of making measurements with satisfactory accuracy, even when the liquid film thickness is very thin because the output signal becomes large as the film thickness decreases. It was originally developed by Fukano (1971) to observe the interfacial structure in co-current gas–liquid two-phase upward flow. Recently, it was used by Deendarlianto et al. (2004) to study the effect of liquid surface tension on the flow pattern and counter-current flow limitation in gas–liquid two-phase flow in an inclined pipe.

In the present report, the experimental results of instantaneous liquid hold-up at the onset of flooding will be presented first. These data will be explained in terms of wave growth and propagation direction of the liquid film. Next, the effects of liquid flow rate and pipe inclination angle on the flooding phenomena will be discussed briefly. Finally, the effect of pipe inclination angle on the onset flooding velocity, wave velocity and

wave frequency at the onset of flooding will be evaluated. The onset of flooding as revealed by the data will be discussed with reference to proposal reported by other investigators.

2. Experimental apparatus and procedures

A schematic diagram of the present experimental apparatus is shown in Fig. 1. A test section of inclined pipe of 16.0 mm inner diameter (D), 2.2 m total length and made of transparent acrylic resin was used to observe the flow phenomena. As shown in Fig. 1, air from compressor entered from the lower end of the inclined pipe and flowed upward through the test section to a separator. Meanwhile, water measured by a digital flow meter, entered from the water inlet and flowed downward in the pipe. To ensure the accuracy, the liquid flow rate was confirmed by collecting the liquid discharged from the lower outlet of test pipe, in a measuring cylinder over a fixed period of time.

The water and air inlets used in the present experiment were the same as that used by Deendarlianto et al. (2002, 2004). The water inlet consisted of a porous section of tube, in order to make the inlet liquid film flow uniform at the point of entry. The air inlet section was made of acrylic resin, providing a conical inlet passage in order to remove the turbulence effect in this area.

In this experiment, liquid film behavior was investigated by measuring the instantaneous local liquid hold-up by using CECM shown in Fig. 2. In the present study, we used seven pairs of liquid hold-up sensors arranged with an axial spacing of 215 mm. Each sensor consists of a pair of brass electrodes, 1 mm in thickness, 5 mm apart from each other, mounted flush with the inner surface of the test pipe. The output signals from these sensors were sent, respectively, through the floating amplifier with high input impedance to a personal computer via an A/D converter. In this experiment, the sampling rate was 1.0 kHz for each experimental run. The details of the experimental apparatus, principle and calibration method can be found in Fukano (1971, 1998).

In order to verify the liquid film behavior recorded on a personal computer by using CECM, visual observations were performed by using two CCD cameras positioned below the water inlet and near the water outlet. The shutter speed was 1/10,000 s.
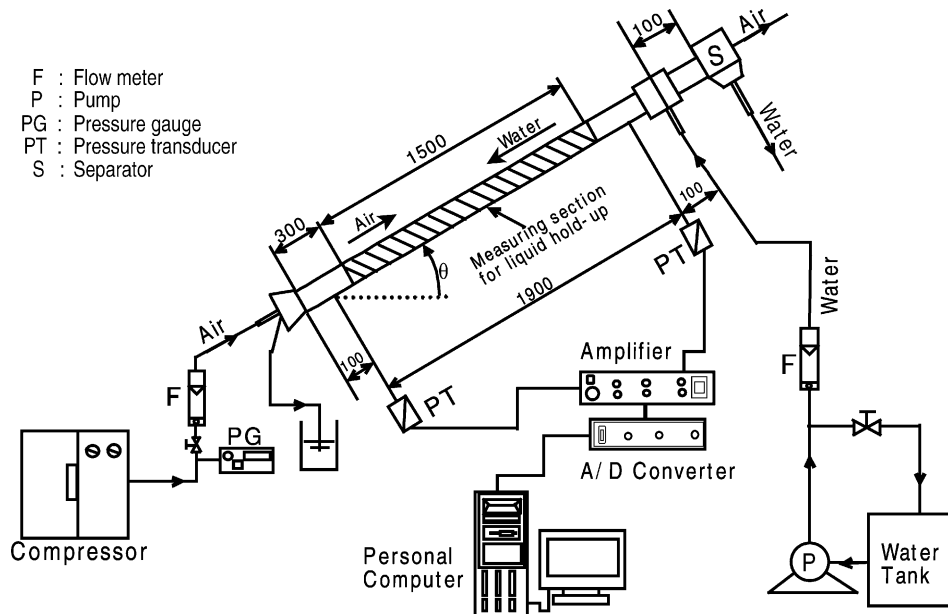

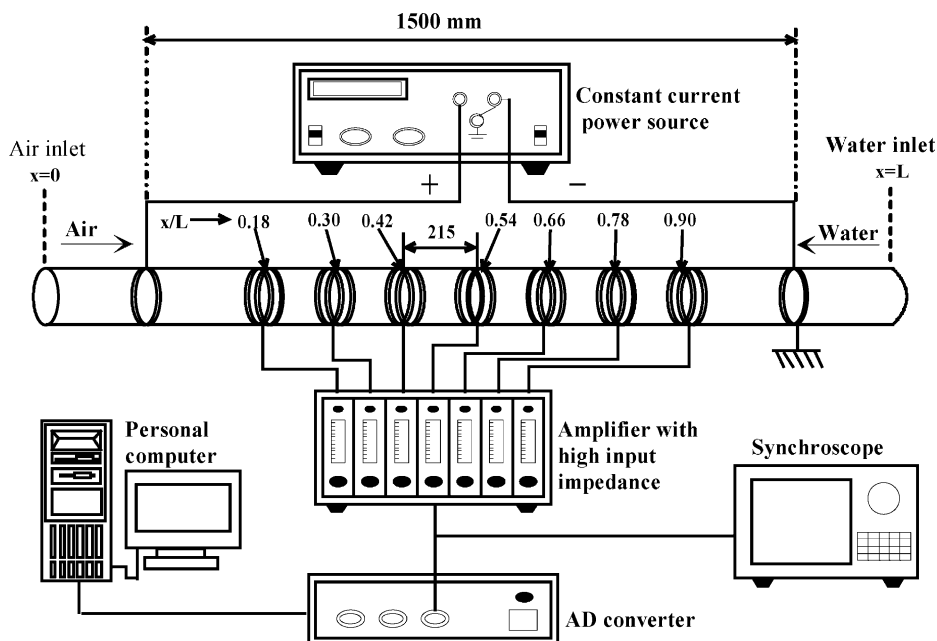Fig. 1. Schematic diagram of experimental apparatus.

Fig. 2. Constant electric current method (CECM).

The experimental conditions were as follows; pipe inclination angles: 30°, 45° and 60° to the horizontal, the range of water superficial velocity: $J_L = 0.03$–0.32 m/s and that of air: $J_G = 0.5$–10 m/s. Working fluids: air and water. Water temperature was approximately 20 °C.

2.1. Experimental procedures to determine the onset of flooding

The onset of flooding was detected as follows. That is, by stepwise increase with a small increment of air-flow rate under a constant water flow rate. We waited for a few minutes to ensure the flow pattern was in a steady state after the change of the airflow rate. At the same time, the pressure gradient, the liquid hold-up and the discharged liquid flow rate were recorded. The onset of flooding was defined as the limiting point of stability of the counter-current flow, indicated by the maximum airflow rate at which the discharged liquid flow rate is equal to the inlet liquid flow rate. This method was used by previous investigators such as by Zabaras and Dukler (1988), Celata et al. (1992) and Deendarlianto et al. (2004).

3. Results and discussion

To simplify the explanation in this paper, we use some abbreviations for the flow characteristics as follows: W, wave; LW, large wave; BW, breakdown of the wave.

3.1. Liquid film behavior at the pipe inclination $\theta = 30°$.

Fig. 3 shows the time variation of liquid hold-up signals recorded by CECM, thus representing the wave progress at the onset of flooding at low water flow rate ($Re_L = 540$). The observed phenomena are as follows:

(1) From Fig. 3, we can see that the wave is formed near the top of the test pipe ($x/L \cong$ unity). The sign of W at $x/L = 0.90$ and $t \approx 1.35$ s indicates the occurrence of this wave. It then propagates downwards and it is clearly seen from the figure that waves shift to the lower right. This means that there is no flow reversal of wave during this period. In addition, the liquid hold-up around the wave increases from $x/L = 0.90$ to 0.18, signifying that the
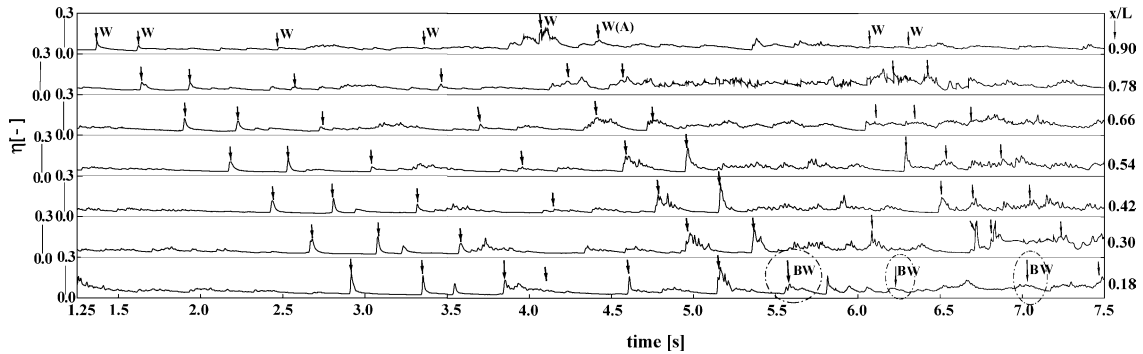
Fig. 3. Time variation of liquid hold-up at the onset of flooding ($Re_L = 540$, $Re_G = 7065$ and $\theta = 30°$).

liquid film thickness around the wave increases with downward movement.

(2) As time goes by, a wave marked as W(A) in this figure is formed near the top of the test pipe at approximately 4.45 s, propagates downwards and is broken up by the airflow at $x/L = 0.18$ and $t \approx 5.65$ s. From an engineering application viewpoint, the breakdown of waves is considered as the onset of flooding because all the liquid supplied cannot flow down smoothly. The sign of BW in the figure indicates this phenomenon. In this period, the corresponding wave at $x/L = 0.3$ and $t \approx 5.35$ s, the height of which is noticeably higher at $x/L = 0.42$, seems to be disappeared when they reached $x/L = 0.18$ and $t \approx 5.65$ s. Consequently, the local liquid hold-up at this wave is smaller than that of $x/L = 0.30$ and $t \approx 5.35$ s. In addition, it is noticed that there is no indication the correspondence waves move upward after BW, that is, there is no reversal of liquid motion even after BW. The definition of liquid motion, here, does not include

the entrainment of liquid droplets. Furthermore, the chaotic flow is limited to a narrow region at the onset of flooding. Consequently, flow instability along the whole pipe as reported by Barnea et al. (1986) was not found in the present experiment.

(3) Next, BW is also detected at the sensor $x/L = 0.18$ and $t \approx 6.35$ s. The reversal motion as characterized by the upper right movement of the correspondent waves does not find in this period also. The process of the wave breakdown under this flow condition is shown in Fig. 4(1), in which the wave appears to form a roll wave near the liquid exit. This wave is broken up into smaller ones with downward movement (Fig. 4(2)) and there are liquid droplets in the gas core (Fig. 4(3)). In addition, a part of these liquid droplets flow upward with the gas phase. The occurrence of the entrainment (liquid droplets) at the onset of flooding supports the results obtained by Dukler and Smith (1979) who defined the flooding to be in progress when the liquid falling film begins to be entrained by upward flowing gas.
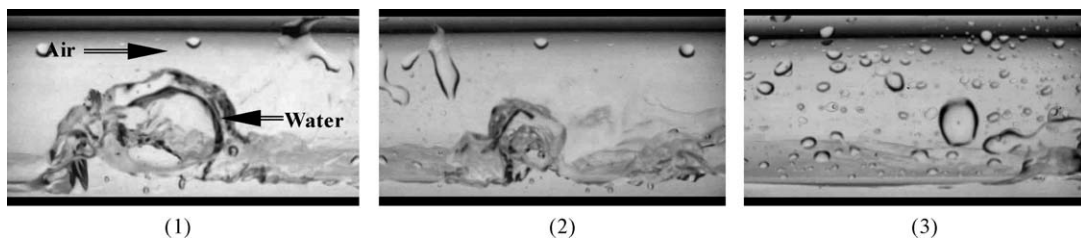

Fig. 4. Breakdown of a wave at the onset of flooding obtained at $x/L \cong 0.18$ ($Re_L = 540$, $Re_G = 7065$, $\theta = 30°$ and frame interval = 1/30 s).
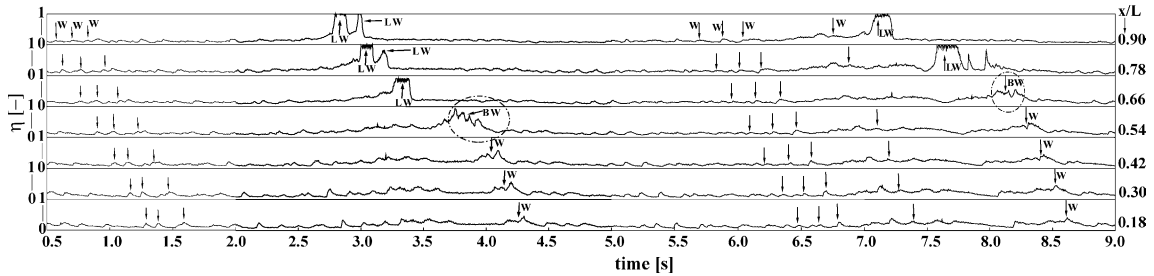
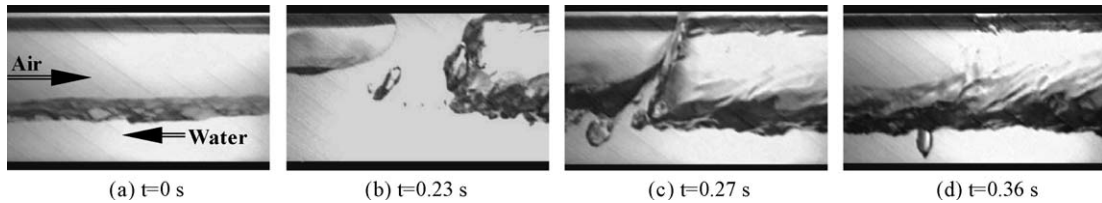Fig. 5. Time variation of liquid hold-up at the onset of flooding ($Re_L = 3970$, $Re_G = 1402$ and $\theta = 30°$).

Fig. 6. Breakdown of a wave at the onset of flooding ($Re_L = 3970$, $Re_G = 1402$ and $\theta = 30°$).

(4) Another parameter that should be considered is the maximum liquid hold-up. Here, that is, about 0.20. This means that the liquid film does not block the whole cross-section of the test pipe.

Fig. 5 shows the time variation of the liquid hold-up by CECM, thus representing the wave progress at the onset of flooding at high liquid flow rate ($Re_L = 3970$ and $\theta = 30°$). It is noted that:

1. The wave assigned as W has been detected at $x/L = 0.90$ and $t \approx 0.55$ s. Thus, wave formation begins at the top of the pipe. This wave also propagates downwards. Here, the liquid hold-up around the wave increases with downward movement and it is again noteworthy that there is no upward motion of the wave during this period.
2. As time goes by, a large wave (LW) is detected occasionally at $x/L = 0.90$ and $t \approx 2.80$ s. It moves downwards until it reaches the sensor $x/L = 0.54$. At this position, it appears to be broken up by the airflow as shown, BW in the figure and produces smaller waves that move downward along the pipe without reversal of motion although the downward velocity becomes low. This phenomenon is repeated continuously and is shown clearly at $x/L = 0.66$ and $t \approx 8.25$ s.
3. The maximum liquid hold-up under this flow condition is about 1.0 at sensors $x/L = 0.90$, 0.78 and 0.66.

Consequently, the liquid lump blocks the whole cross-section of the test pipe close to the water inlet. To understand this phenomenon, visual observation taken by a high-speed video camera and the air inlet pressure measurement were done simultaneously around the blockage and the breakdown of the wave. The results are shown in Figs. 6 and 7. Fig. 6(a) shows the interfacial behavior before the blockage process. However, it appears to be small waves. The corresponding point of this figure is marked as (a) in Fig. 7 and it can be seen that the air inlet pressure is very low. As time goes by, a large wave occurs
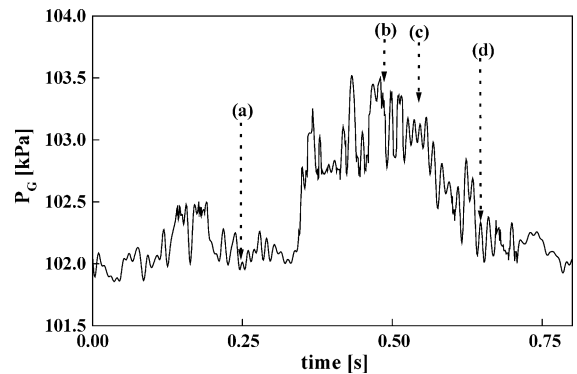

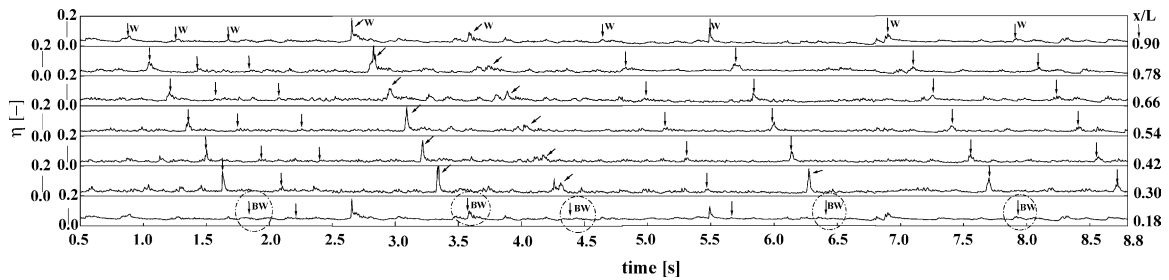Fig. 7. Time variation of the air inlet pressure ($Re_L = 3970$, $Re_G = 1402$ and $\theta = 30°$).

Fig. 8. Time variation of liquid hold-up at the onset of flooding ($Re_L = 540$, $Re_G = 8168$ and $\theta = 45°$).

and blocks the tube whole cross-section. This phenomenon is shown in Fig. 6(b). It is marked in Fig. 7 with (b). It can be seen that the air inlet pressure becomes very high. This means that the blockage process compresses the airflow in the pipe and makes the air inlet pressure increase. Hereinafter, the supply of airflow reduces the length of the liquid slug and breaks it (Fig. 6(c and d)). Fig. 7 indicates that the air inlet pressure becomes smaller during this period.

Some additional remarks are added at this point, to the flow behavior at the onset of flooding in the pipe inclination angle of $\theta = 30°$:

1. BW is observed close to the water outlet at lower liquid flow rate. BW appears, however, at higher location in the pipe with higher water flow rate. That is, the location of the BW moves to the upper part of the test pipe with the increasing liquid flow rate.
2. The liquid slug does not block the whole pipe cross-section at lower liquid flow rate, while such the blockage is observed in the top half of the test pipe at high water flow rate.
3. The inclination angle plays a significant role to the flooding mechanism involving the occurrence of BW and the generation of liquid droplets in the airflow. From this observation, it is concluded that the occurrence of BW and liquid droplet are integral phenomena of the initial stage of flooding in counter-current flow.

3.2. Liquid film behavior at the pipe inclination $\theta = 45°$

At higher pipe inclination angle ($\theta = 45°$) and low water flow rate ($Re_L = 540$), the time variation of liquid

hold-up at the onset of flooding is given in Fig. 8. Close inspection of this figure reveals that:

1. Waves are initiated at the top of the tube and propagate downwards in the same way as the case of $\theta = 30°$. The liquid film thickness around the wave increases as the wave moves downstream. This fact is shown clearly in the figure, in which the liquid hold-up around the wave increases. This trend is indicated by the increasing of the top of the wave as clearly seen from the traces detected at $x/L = 0.90$ to 0.18.
2. As the time proceeds, BW occurs at the bottom of the test pipe, for example, $x/L = 0.18$ and $t \approx 1.78$ s. Further evidence of this phenomenon is also shown at $x/L = 0.18$ and $t \approx 3.60$, 4.40, 6.35 and 7.85 s, respectively, in which the process of wave growth and breakdown is repeatedly observed. It is also evident that the reversal of wave motion does not occur during this period. A sample of the sequence picture showing the breakdown of the wave under this flow condition is shown in Fig. 9.
3. The maximum of the liquid hold-up along the test pipe was about 0.17. It means that the wave did not block the test pipe. This result is similar to that of $\theta = 30°$. Thus, flow behavior at the onset of flooding in low water flow rate shows little change if the pipe inclination angle increases from 30° to 45°.

In the case of higher water flow rate ($Re_L = 3970$ and $\theta = 45°$), the time variation of the liquid hold-up at the onset of flooding is shown in Fig. 10. In comparison with Fig. 5 taken under the same water flow rate but the pipe inclination angle $\theta = 30°$, we notice the phenomenon is similar. That is, the maximum of the liquid hold-up was about 1.0 at $x/L = 0.90$, signifying that the liquid film blocks the overall cross-section of
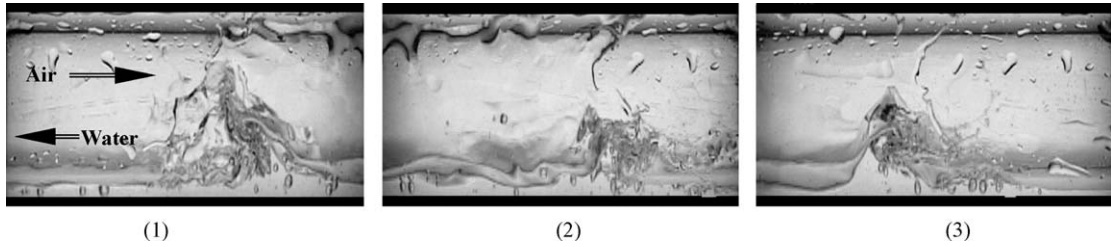
Fig. 9. Breakdown of wave at the onset of flooding of $Re_L = 540$, $Re_G = 8168$ and $\theta = 45°$ (frame interval was 1/30 s).

the test pipe at this position. In addition, BW arises at similar locations, is detected by sensors ranging from $x/L = 0.78$ to 0.54. From these results, it is concluded that the flow behavior at the onset of flooding does not fundamentally change if the pipe inclination angle changes from 30° to 45° even in high liquid flow rate.

3.3. Liquid film behavior at the pipe inclination $\theta = 60°$

Fig. 11 shows the time variation of liquid hold-up at low water flow rate ($Re_L = 540$) when the pipe inclination angle θ was 60°. Close inspection of the figure reveals that the flow characteristics change a little with increasing inclination. The wave is also formed at the top of the test pipe as shown, for example, by $x/L = 0.90$ and $t \approx 0.48$ s in Fig. 11 and the reversal of wave motion also does not occur. Here, the maximum of the liquid hold-up along the pipe is about 0.19, so there is no blockage process in the pipe. Meanwhile, BW is not observed in the range from $x/L = 0.18$ to 0.90. According to the visual observation, BW occurred at just upstream of the air inlet, $x/L \leq 0.05$. The example of BW at this position is shown in Fig. 12.

Finally, the time variation of liquid hold-up at high water flow rate ($Re_L = 3970$ and $\theta = 60°$) shown in Fig. 13 will be discussed. The following features are noteworthy:
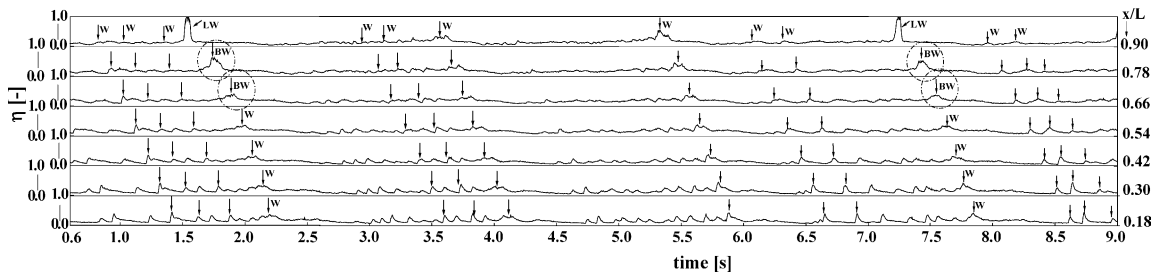

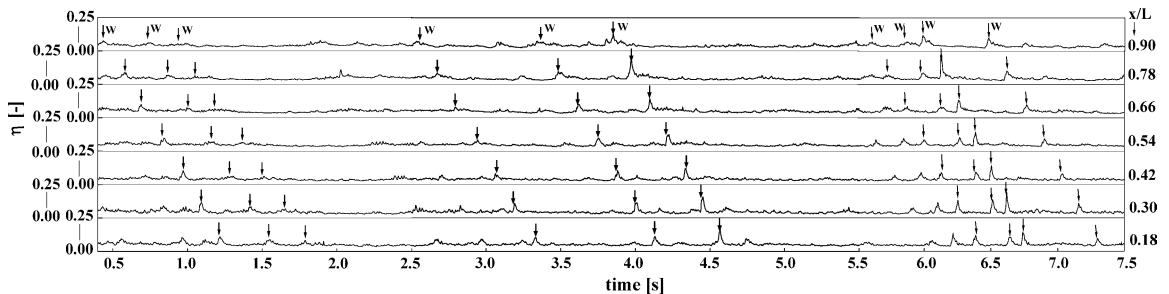Fig. 10. Time variation of liquid hold-up at the onset of flooding ($Re_L = 3970$, $Re_G = 2200$ and $\theta = 45°$).

Fig. 11. Time variation of liquid hold-up at the onset of flooding ($Re_L = 540$, $Re_G = 6704$ and $\theta = 60°$).

Fig. 12. Breakdown of the wave at the onset of flooding of $Re_L = 540$, $Re_G = 6704$ and $\theta = 60°$ (frame interval was 1/30 s).

1. The wave is initiated at the top of the test section and propagates downwards. Here, the liquid hold-up around the wave increases with downward movement as indicated by the increasing height at successive sensors. BW is found at the lower position of the test pipe ($x/L = 0.18$). From the previous discussion, it is noted that the BW occurs at the upper part of the test pipe (x/L ranged from 0.54 to 0.78) when the pipe inclination angles are $\theta = 30°$ and $45°$. On the other hand, the initiation of the BW occurs at a lower position when the pipe inclination angle is increased to $\theta = 60°$.

2. The maximum of the liquid hold-up at this flow condition is 0.43. So, the liquid does not block the cross-section of the test pipe. In the previous discussion, it is noted that the liquid blocked the whole cross-section of the test pipe when the pipe inclinations were $\theta = 30°$ and $45°$ at high water flow rate ($Re_L = 3970$). Furthermore, Karimi and Kawaji reported that the liquid film did not block the cross-section of the pipe when the pipe inclination angle was $\theta = 90°$. From these results, it is possible to conclude that the blockage process disappears when the pipe inclination approaches the vertical position, because the liquid flow is more accelerated by the

gravity force in the case of higher inclination angle and the liquid hold-up becomes small.

3.4. Flooding mechanisms

From the observation of the liquid film behavior near the onset of flooding using the combination of visual observation and time variation of liquid hold-up, two mechanisms of flooding phenomena are identified. Those are lower flooding and upper flooding, which depend on the position where the flooding is initiated at the lower or upper locus of the test section. Their behaviors are described below.

3.4.1. Lower flooding

This mechanism was found to occur at the pipe inclination $\theta = 60°$. However, at pipe inclinations $\theta = 30°$ and $45°$, the lower flooding is found to occur only at water flow rate $Re_L < 3970$. The formation of wave near the water inlet initiates this mechanism. The wave increases progressively in size with downward propagation. When the wave height reaches a certain value, it begins to be broken up by the airflow near the water outlet. The process of wave growth and breakdown is repeated continuously at approximately fixed locations
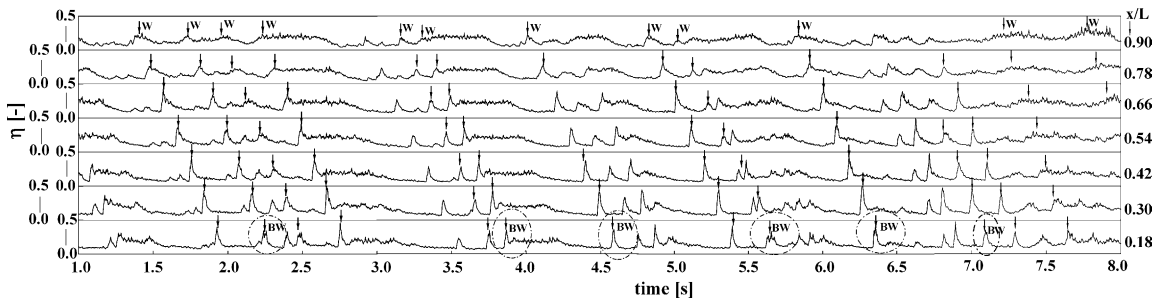

Fig. 13. Time variation of liquid hold-up at the onset of flooding ($Re_L = 3970$, $Re_G = 2567$ and $\theta = 60°$).

(x/L ranged from 0.0 to 0.5). At this stage, the entrainment liquid droplets can be observed. Both the visual observation and the time variation of liquid hold-up detected along the pipe did not reveal any upward moving waves and the liquid film never completely blocked the pipe cross-section.

This mechanism is similar to those proposed by Karimi and Kawaji (2000) and Zabaras and Dukler (1988) who examined the liquid film behavior at the onset of flooding in vertical pipes. They found that the interfacial waves propagate downwards with considerable velocity. Furthermore, Karimi and Kawaji reported that the measured velocity profiles did not show any indication of flow reversal in the liquid film at the onset of flooding and that only a slight reduction in velocity was observed within a short axial region very close to the gas–liquid interface. Meanwhile, this result is partly in agreement with Mouza et al. (2003) who performed flooding experiment in inclined small diameter pipes. They concluded that the waves reversed their flow direction at the onset of flooding and disintegrated, to some extent, into small droplets. The occurrence of these droplets is also recorded visually in our experiment, but we did not find any evidence of the reversal motion of the waves. It is considered that the use of visual identification and the different definition of flooding in the individual researches have led to these different conclusions. On the other hand, different phenomena may be created because of using a different pipe diameter (16 mm versus 9 mm) as reported by Vijayan et al. (2002).

3.4.2. Upper flooding

Upper flooding was found to occur at higher water flow rate (($Re_L \geq 3970$) when the pipe inclinations were $\theta = 30°$ and $45°$). This was initiated by the sudden formation of a large wave that completely blocks the whole cross-section of the test pipe near the water inlet. Such a large wave, water lump propagated downwards for a short distance. Due to the continuity of the up going airflow, then the water lump is broken into a number of droplets at this position (x/L ranged from 0.5 to 1.0). The process of wave growth and breakdown was repeated continuously and was observed at the upper half of the test section. The wave, however, propagated downwards normally. From the time variation of liquid hold-up and visual observation, we also did not find any
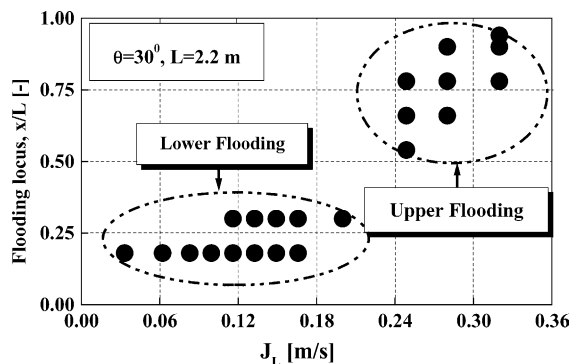

Fig. 14. Typical result of flooding locus ($\theta = 30°$).

upward motion of waves. From the above explanation, it is concluded that the upper flooding is initiated by a localized formation of liquid slug in the upper half of pipe length. In order to convince the obtained flooding mechanisms, typical result of flooding locus is given in Fig. 14. This figure demonstrates that the flow mechanisms at the onset of flooding are divided into two groups as proposed in the present paper.
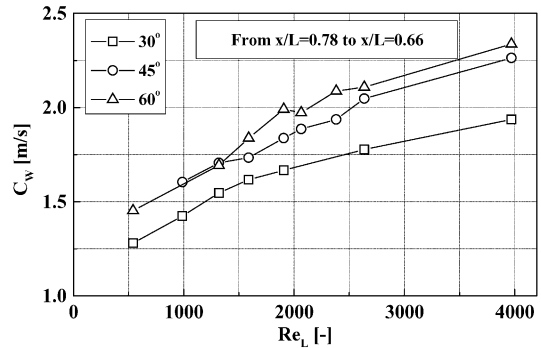
3.5. Wave velocity and wave frequency

The wave velocity was determined from the delay time of a maximum peak in the cross-correlation function between any two signals by the CECM located at seven different locations with each separation of 215 mm. From the results shown in Fig. 15, it is revealed that the values of the wave velocity at the onset of flooding are positive, signifying that waves travel downwards, which is in agreement with Zabaras and Dukler (1988) and Karimi and Kawaji (2000). This fact supports the proposed flooding mechanism in the present paper, i.e., there is no reversal motion at the onset of flooding. That is, the wave travels downward with the gravitational force balancing with shear force by the airflow and base film flow. Furthermore, the wave velocity at the onset of flooding increases with the pipe inclination.
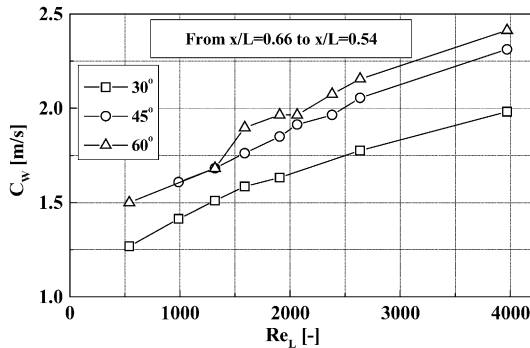
Fig. 16 shows the variation of the wave frequency at the onset of flooding plotted as a function of water Reynolds number and pipe inclination. It was determined by counting the number of waves from the traces of the time variation of liquid hold-up at $x/L = 0.18$. It was also checked by the wave frequency as observed
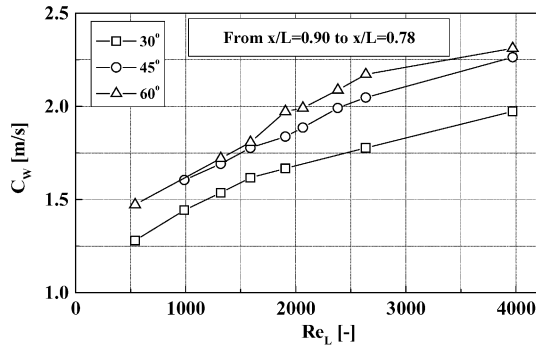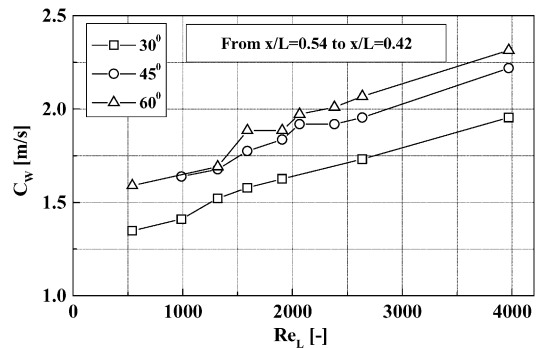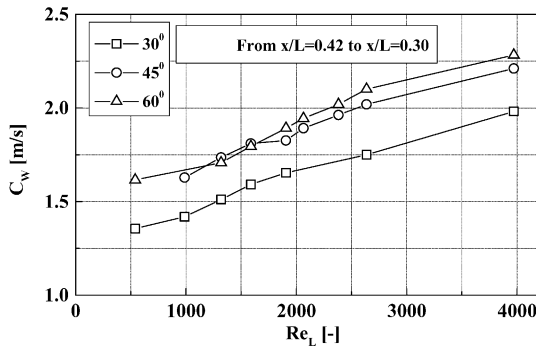
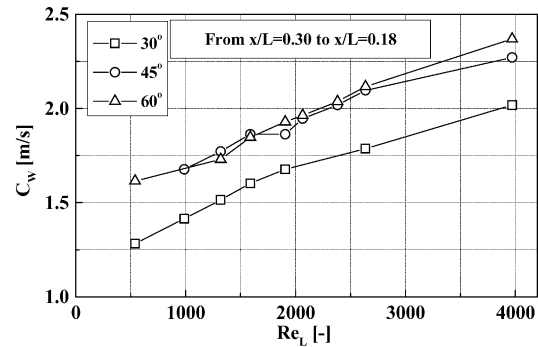(a) From x/L=0.90 to x/L=0.78

(b) From x/L=0.78 to x/L=0.66

(c) From x/L=0.66 to x/L=0.54

(d) From x/L=0.54 to x/L=0.42

(e) From x/L=0.42 to x/L=0.30

(f) From x/L=0.30 to x/L=0.18

Fig. 15. Wave velocity at the onset of flooding.

on the video recording. As can be seen in Fig. 16, the wave frequency increases with the pipe inclination in the case of higher liquid flow rate. In the case of pipe inclinations $\theta = 30°$ and $60°$, a reduction in the wave frequency is observed for $Re_L > 2500$. Meanwhile, when the pipe inclination is $45°$, the wave frequency increases as the liquid Reynolds number increases. The

reasons for this effect are not fully understood, but it probably occurs because of the change in the liquid film distribution with the pipe inclination and liquid flow rate. However, from these results, it is concluded that the pipe inclination angle and liquid Reynolds number affect the wave frequency at the onset of flooding.
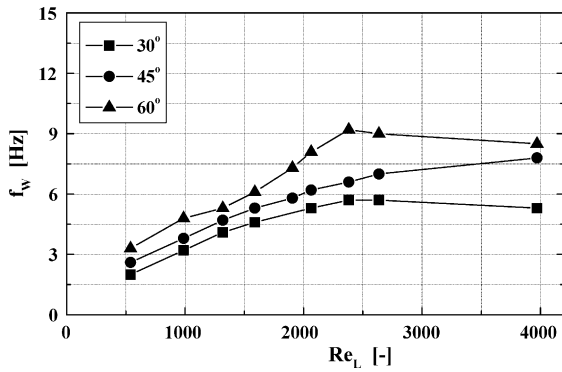
Fig. 16. Wave frequency at the onset of flooding.

3.6. The onset of flooding velocity

Wallis (1969) proposed the dimensionless number, J_K^*, in terms of the gas and liquid superficial velocities to predict the onset of flooding in a vertical pipe. It is defined as follows:

$$J_K^* = J_K \sqrt{\frac{\rho_K}{gD(\rho_L - \rho_G)}} \qquad (1)$$

where subscript K indicates gas and liquid phases, ρ the density and D is the inner pipe diameter. The correlation is expressed as,

$$(J_G^*)^{1/2} + m(J_L^*)^{1/2} = C \qquad (2)$$

The constants m and C are determined by the experiment. In the case of vertical pipes, C lies between 0.88 and 1.0.
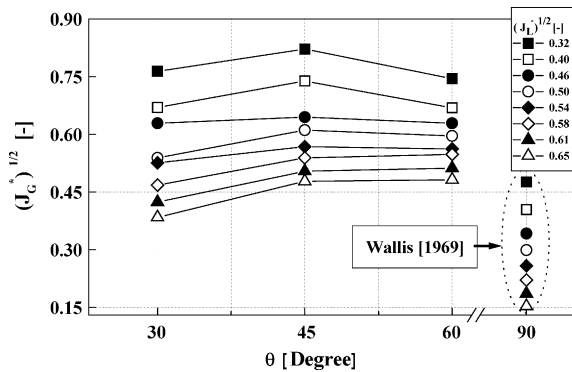

Fig. 17. Effect of the pipe inclination on the onset of flooding velocity.

Fig. 17 shows the effect of pipe inclination on the onset of flooding velocity. As shown in this figure, the trend is complicated. That is, $(J_G^*)^{1/2}$ at the onset of flooding takes the maximum value at about $\theta = 45°$ in the region of $(J_L^*)^{1/2} < 0.58$, while it takes the maximum value at the higher pipe inclination in the region of $(J_L^*)^{1/2} \geq 0.58$. It is easily considered that the important parameters in these trends are the liquid film thickness and gravity force. However, in order to clarify the physics of this, further investigation on the liquid film thickness distribution in counter-current gas–liquid two-phase flow in an inclined pipe is needed. On the other hand, $(J_G^*)^{1/2}$ obtained by Wallis (1969) for a vertical pipe takes smaller values than those in inclined pipes. In addition, in the range of pipe angles tested, the present results show that $(J_G^*)^{1/2}$ at the onset of flooding decreases as water flow rate increases.

Fig. 18 shows a comparison of the present results with the results obtained by Hewitt (1977), Barnea et al. (1986), Zapke and Kroger (1996), Wongwises (1998) and Mouza et al. (2003). Fig. 18(a and b) correspond, respectively, to the cases of $\theta = 30°$ and $60°$. As shown in these figures, the present results agree well as a whole with the data by Hewitt in the both cases of $\theta = 30°$ and $60°$. However, Hewitt data underestimate compared to the present result in case of $\theta = 60°$ and $(J_L^*)^{1/2} \geq 0.5$. On the other hand, the data by Barnea et al., Mouza et al. and Zapke and Kroger are considerably higher than the present data in the both cases, $\theta = 30°$ and $60°$. This may be due to the difference of the pipe diameters and the definition of the onset of flooding as noted previously. That is, the inner diameter of the present test pipe was 16 mm, and those of Barnea et al., Mouza et al. and Zapke and Kroger were, respectively, 51, 9 and 30 mm.

The data of $(J_G^*)^{1/2}$ by Wongwises are significantly lower than those of Zapke and Kroger, and Hewitt as clearly shown in Fig. 18(b), although it was obtained under similar conditions such as the pipe diameter, pipe inclination, working fluids and experimental ranges. This comparison indicates that there is no agreement about the onset of flooding velocity among the data obtained by these researchers, although they conducted experiments under similar conditions. This suggests that further research is needed on the mechanism of the onset of flooding in order to develop a detail theoretical flooding model for an inclined pipe under a clear understanding of the definition of the onset of flooding.
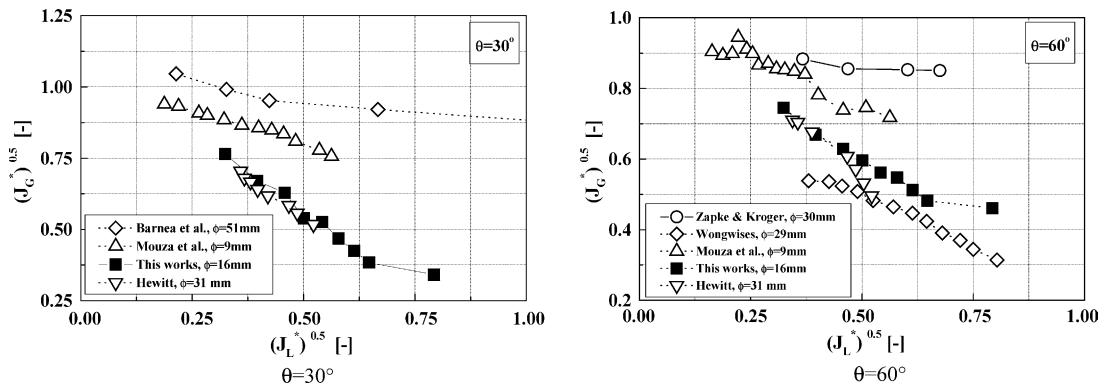
Fig. 18. Comparison of the present results with other flooding data.

4. Conclusions

The effects of the liquid flow rate and pipe inclination on the liquid film behavior at the onset of flooding in an inclined pipe were investigated experimentally. The working fluids were air and water, the inner pipe diameter and the pipe length were, respectively, 16 mm and 2.2 m. The results are summarized as follows:

1. The time variation of liquid hold-up signals detected along the pipe by using the constant current electric method has been successfully used to identify the flooding mechanisms. The identified flooding mechanisms are the lower flooding and the upper flooding.
2. In the case of the lower flooding, the wave is formed in an upper part of the pipe and propagates downwards. At a certain wave height, the wave is broken up by the airflow in the bottom half of the pipe length. In this mechanism, the wave never completely blocks the cross-section of test pipe. In addition, no upward motion of the wave is observed in the present experiment. Furthermore, this mechanism occurs at lower liquid flow rate and high pipe inclination.
3. In the case of upper flooding, the wave is formed in upper position of test pipe and propagates downwards. The breakdown of this wave occurs within the upper half of the pipe length after the wave blocks the whole cross-section of the test pipe. In addition, this mechanism occurs at higher liquid flow rate and low pipe inclination.

4. From the wave velocity data at the onset of flooding, it is found that there is no upward motion during either lower and upper flooding.
5. The velocity at the onset of flooding takes the maximum value at pipe inclination $\theta = 45°$ in the region of low superficial liquid velocity and it shifts to the higher inclination angles in the region of high superficial liquid velocity.

References

Barnea, D., Ben Yoseph, N., Taitel, Y., 1986. Flooding in inclined pipe: effect of entrance section. Can. J. Chem. Eng. 64 (2), 177–184.

Celata, G.P., Cumo, M., Setaro, T., 1992. A data set of flooding in circular tubes. Exp. Therm. Fluid Sci. 5, 437–447.

Deendarlianto, Ousaka, A., Kariyasaki, A., Kusano, K., 2002. Flooding phenomena for air–water two-phase flow in inclined pipe: effect of pipe inclination on the onset of flooding. In: 5th JSME–KSME Fluids Engineering Conference, Paper No. 10j_11, Nagoya, Japan (CD-ROM).

Deendarlianto, Ousaka, A., Kariyasaki, A., Fukano, T., Konishi, M., 2004. The effects of surface tension on the flow pattern and counter-current flow limitation (CCFL) in gas–liquid two-phase

flow in an inclined pipe. Jpn. J. Multiphase Flow 18 (4), 337–350.

Dukler, A.E., Smith, L., 1979. Two-phase interactions in countercurrent flow: studies of the flooding, USNRC, NUREG/CR-0617.

Fukano, T., 1971. Characteristics of pulsation of gas–liquid two-phase upward flow. Dr. Thesis, Kyushu University (in Japanese).

Fukano, T., 1998. Measurement of time varying thickness of liquid film flowing with high speed gas flow by a constant electric current method (CECM). Nucl. Eng. Des. 184, 363–377.

Hewitt, G.F., 1977. Influence of end conditions, tube inclination and physical properties on flooding in gas–liquid flow. UKAEA Report HTFS-RS222.

Imura, H., Kusuda, H., Funatsu, S., 1977. Flooding velocity in a counter-current annular two-phase flow. Chem. Eng. Sci. 32, 79–87.

Karimi, G., Kawaji, M., 2000. Flooding in vertical counter-current flow. Nucl. Eng. Des. 200 (1), 95–105.

McQuilland, K.W., Whalley, P.B., 1985. Flooding in vertical two-phase flow. Int. J. Multiphase Flow 11 (6), 741–760.

Mouza, A.A., Paras, S.V., Karabelas, A.J., 2003. Incipient flooding in inclined tubes of small diameter. Int. J. Multiphase Flow 29 (9), 1395–1412.

Vijayan, M., Jayanti, S., Balakrishnan, A.R., 2002. Experimental study of air–water counter-current annular flow under post-flooding conditions. Int. J. Multiphase Flow 27 (1), 51–67.

Suzuki, S., Ueda, T., 1977. Behavior of liquid films and flooding in counter-current two-phase flow. Part 1. Flow in circular tubes. Int. J. Multiphase Flow 3 (6), 517–532.

Wallis, G.B., 1969. One-Dimensional Two-Phase Flow. McGraw-Hill, New York, pp. 336–345.

Wongwises, S., 1998. Effect of inclination angles and upper end conditions on countercurrent flow limitation in straight circular pipes. Int. Commun. Heat Mass Transfer 25 (1), 117–125.

Zabaras, G.J., Dukler, A.E., 1988. Counter-current gas–liquid annular flow, including the flooding state. AIChE J. 34 (3), 389–396.

Zapke, A., Kroger, D.G., 1996. The influence of fluid properties and inlet geometry on flooding in vertical and inclined tubes. Int. J. Multiphase Flow 22 (3), 461–472.